INFLUENCE OF POLYPHENOLS ON THE INTEGRATED POLYPHENOL-MAILLARD REACTION HUMIFICATION PATHWAY AS CATALYZED BY BIRNESSITE

A. G. Hardie,[1] J. J. Dynes,[2,3] L. M. Kozak[1] and P. M. Huang[1*]

[1] Department of Soil Science, University of Saskatchewan, 51 Campus Drive, Saskatoon, SK, S7N 5A8, Canada
[2] Environment Canada, 11 Innovation Place, Saskatoon, SK, S7N 3H5, Canada.
[3] Department of Chemistry, McMaster University, 1280 Main St. W., Hamilton, ON, L8S 4M1, Canada.

Received May 29, 2007; in final form October 29, 2007; Accepted November 15, 2007

ABSTRACT

The significance of linking the Maillard reaction and polyphenol pathway as promoted by birnessite (δ-MnO_2) into an integrated humification pathway has previously been demonstrated using a system containing catechol, glucose and glycine. The kinds and relative abundance of biomolecules (polyphenols, sugars and amino acids) involved in the proposed integrated humification pathway substantially vary with natural vegetation, microbial populations and activity, and the environment. Therefore, the objective of our study was to examine the effect of two structurally different polyphenols, namely, pyrogallol and resorcinol, in the integrated polyphenol-Maillard reaction system on the humification processes as catalyzed by birnessite. A number of experiments with an increasing concentration of polyphenol (pyrogallol or resorcinol) to a fixed molar ratio of Maillard reagents (glucose and glycine) were conducted under environmentally relevant conditions, and subsequently the degree of humification and the nature of the products formed were examined using XRD, visible absorption, FTIR and C K-edge and Mn L-edge NEXAFS spectroscopies. Our results clearly demonstrate that the structure and functionality of pyrogallol and resorcinol and their molar ratio to Maillard reagents in the polyphenol-Maillard reaction system not only significantly affect the humification processes but also the formation of rhodochrosite ($MnCO_3$). The integrated pyrogallol-Maillard reactions systems formed the least $MnCO_3$ and were more enriched in organic components in the solid phase than the integrated resorcinol-Maillard reaction system. The position and/or number of OH groups on the benzene ring of the polyphenols substantially affects the extent of direct electron transfer reactions, which impacts the reductive dissolution of birnessite, and oxidative polymerization and cleavage of biomolecules. This in turn affects the nature of the humic substances formed. The findings obtained in this study are of fundamental significance in understanding the importance of the nature and abundance of biomolecules in influencing abiotic humification pathways and carbonate formation in natural environments.

Keywords: Abiotic humification; polyphenol-Maillard reaction pathway; pyrogallol; resorcinol; birnessite; NEXAFS

1. INTRODUCTION

Humic substances are formed through both selected preservation processes and biotic (enzymatic) and abiotic (mineral) catalytic synthesis mechanisms [1-3]. The Maillard reaction, involving condensation reactions between sugars and amino acids [4], is regarded as an important pathway in natural humification processes [5]. The appeal of the Maillard reaction in understanding humification processes lies in the two proposed precursors (sugars and amino acids) being among the most abundant biomolecules of terrestrial and aquatic environments [6]. Further support is lent by the presence of humic substances in marine environments where carbohydrates and proteins, because of their abundance, are more probable precursors of humic substances than lignin or phenolic polymers [5].

Although the potential energy barrier of the Maillard reaction is high [7], Jokic et al. [8] reported that birnessite (δ-MnO_2), which is commonly present in the environment, decreases the energy barrier and thus enhances the reaction rates by one to two orders of magnitude at environmentally relevant temperatures (25 and 45°C) and at neutral pH. Furthermore, Jokic et al. [9] clearly showed, using N

* Corresponding author: Department of Soil Science, University of Saskatchewan, 51 Campus Drive, Saskatoon, SK, S7N 5A8, Canada. Phone: +306-966-6838, fax: +306-966-6881, e-mail: <pmh936@mail.usask.ca>

K-edge NEXAFS, that the Maillard reaction involving glucose and glycine, catalyzed by birnessite under environmentally relevant conditions not only produces heterocyclic N but also a significant amount of amide N. This provides an explanation for one of the pathways of formation of heterocyclic N and amide N found in humic substances in the environment. Abundant scientific evidence at the molecular level shows the significance of the polyphenol pathway in humification [1, 2, 10, 11].

The surfaces of soil metal oxides, particularly redox active oxides such as birnessite, are very effective in promoting the oxidative polymerization of phenolic compounds. They can act as Lewis acids by accepting electrons from hydroxyphenolics, leading to the formation of highly reactive semiquinone radicals that readily undergo coupling reactions with other semiquinones, phenolics, amino acids or existing humus [11].

Sugars, amino acids and polyphenols coexist in soil solutions and natural waters. Therefore, in nature it is most likely that the Maillard reaction and polyphenol pathways do not occur separately but rather interact with each other. Jokic et al. [12] were the first to study an integrated Maillard reaction and polyphenol pathway of humification using catechol, glucose and glycine as reagents and birnessite as the catalyst. Their data showed that the ubiquitous soil mineral birnessite significantly accelerates humification processes in an integrated polyphenol-Maillard reaction system under pH and temperature conditions typical of natural environments.

Haffenden and Yaylayan [13] showed that adding a mixture of polyphenols (catechol, resorcinol, hydroquinone & pyrogallol) to an equimolar solution of glucose and glycine and then heating the mixtures results in a significant enhancement of the degree of browning in the system compared to the heated glucose and glycine reaction system alone. These results support the findings of Jokic et al. [12] that the integrated polyphenol-Maillard reaction system is more effective in generating humic materials than the Maillard reaction alone. The kinds and relative abundance of biomolecules (that is sugars, amino acids and polyphenols) substantially vary with natural vegetation, microbial populations and activity, and the environment [1, 14]. Sources of phenols include lignin degradation, microbial metabolites, plant root exudates and tannins [1]. The types of phenols produced vary substantially with the organisms involved. For instance, lignin degradation by brown-rot fungi gives rise primarily to catechol-type constituents [15], whereas the phenols synthesized by fungi such as *E. Nigrum* differ in that they contain resorcinol and resorcinol-type constituents, which do not occur in lignin degradation products [16].

Both lignin degradation and microbial synthesis processes give rise to pyrogallol and pyrogallol-type polyhydroxyphenolic acids [1]. It has been shown that there are significant differences in the reactivity of polyphenols in relation to their structure, most importantly the positions and number of the OH groups on the benzene ring [17-19]. Stone and Morgan [18] found that the diphenols catechol (*ortho*-OH group), resorcinol (*meta*-OH group) and hydroquinone (*para*-OH group) are able to reduce and dissolve Mn(III, IV) oxide in the following order catechol > hydroquinone > resorcinol. They concluded that the reducing ability of diphenols is based on their ability to form a surface complex with the Mn oxide prior to electron transfer. Thus *ortho*- and *para*-OH groups are readily able to form surface complexes with Mn(III, IV) oxide while the formation of surface complexes with a diphenol containing a *meta*-OH group is much less favorable.

Shindo [20] studied the polymerization of various polyphenols by birnessite, and found that pyrogallol yielded far more humic acid (1145 mg C/g oxide) than catechol (438 mg C/g oxide) or resorcinol (240 mg C/g oxide). Wang and Huang [19] reported that pyrogallol, with three OH groups directly next to one another, is far more easily cleaved by nontronite (Fe-bearing smectite) than the diphenols catechol or hydroquinone. This is directly related to the ability of the polyphenol to form a direct surface complex with the mineral surface, which facilitates electron transfer and subsequent cleavage.

Wang and Huang [19] concluded that the greater the ease of ring cleavage of a polyphenol, the more CO_2 is released and the more aliphatic fragments are incorporated into the resultant humic substances. Furthermore, Wang and Huang [21, 22] demonstrated the substantial ring cleavage of pyrogallol by birnessite. Remaining to be studied is the effect that the kind of polyphenol has on the integrated polyphenol-Maillard reaction humification processes, as Jokic et al. [12] only investigated the catechol-glucose-glycine system.

Therefore, the objective of this study was to investigate the effect of two structurally different polyphenols, namely resorcinol (1,3-dihydroxy-benzene) and pyrogallol (1,2,3-trihydroxybenzene) (Fig. 1) on the integrated polyphenol-Maillard reaction (glucose and glycine) humification pathway as catalyzed by birnessite. This was carried out by examining and comparing the degree of humification and the nature of the reaction products (humic acid and the organo-mineral phase) from the Maillard reaction, resorcinol-Maillard, pyrogallol-Maillard, and resorcinol- and pyrogallol-only systems. Our ultimate

goal is to elucidate the importance of the nature and abundance of biomolecules in influencing abiotic humification pathways and related reaction products in natural environments.

(a) (b)

Figure 1 Chemical structures of (a) resorcinol and (b) pyrogallol.

2. MATERIALS AND METHODS

2.1. Materials

Birnessite (δ-MnO_2) was synthesized by a method described by McKenzie [23] that involves reducing boiling $KMnO_4$ by slowly adding concentrated HCl. The precipitate was washed by repeated filtration using distilled deionized water (henceforth referred to as water) on a 0.1 μm pore Millipore membrane filter, until the wash water tested free of chloride ($AgNO_3$ test). It was then freeze-dried, and then lightly ground with a mortar and pestle. The synthesized birnessite was characterized by X-ray diffraction (XRD) (Rigaku Rotaflex 200SU, Tokyo, Japan), Fourier transform infrared (FTIR) spectroscopy (Bruker Equinox 55, Ettlingen, Germany), Mn L-edge near edge X-ray absorption fine structure (NEXAFS) at the Canadian Light Source (Saskatoon, SK, Canada) on the SGM (spherical grating monochromator) beamline and BET specific surface area analysis (Quantachrome Autosorb-1, Syosset, NY, USA) using N_2 gas. Pyrogallol, resorcinol, D-glucose (Sigma-Aldrich ACS reagent grade >99%) and glycine (Sigma Ultra pure grade >99%) were obtained from Sigma-Aldrich Canada Ltd (Oakville, ON, Canada). Pure manganese carbonate and oxides, $MnCO_3$ (99.99%), MnO (>99%), Mn_2O_3 (>99%), and MnO_2 (>99%), were obtained from Sigma-Aldrich to use as reference compounds in the XRD and NEXAFS studies. Elliot soil (1S102H) and Florida Peat (1S103H) humic acid standards were purchased from the International Humic Substances Society (IHSS), St. Paul, MN, USA, and used in the C K-edge NEXAFS study.

2.2. Reaction procedures

2.2.1 Incubation Experiment

Sterile conditions were maintained throughout the experiment in order to establish the role of abiotic processes. All glassware, birnessite, water and apparatus were autoclaved prior to the experiments. In addition to this, thimerasol (an antibacterial agent) was added to each flask (0.02%, w/v final volume) before any of the reagents were added. Thimerasol does not affect the oxidation process of phenolic compounds [24]. To investigate the effect of the molar ratio of pyrogallol or resorcinol to Maillard reagents, a number of experiments were employed with increasing amounts (0; 1.25; 2.5; 12.5; 25.0; 50.0; 100 mmoles) of pyrogallol or resorcinol added to a fixed molar ratio of Maillard reagents (50 mmole glucose + 50 mmole glycine) using birnessite as catalyst. Two and a half grams of birnessite were suspended in each of the reaction solutions in a 250 mL flask. There were also selected control experiments in which birnessite was absent, i.e., the pyrogallol or resorcinol only systems (50 mmole pyrogallol/resor-cinol) and the pyrogallol or resorcinol integrated equimolar polyphenol-Maillard system (50 mmole glucose + 50 mmole glycine + 50 mmole pyrogallol/resorcinol).

All the reaction systems were adjusted to an environmentally relevant pH 7.0 using 0.1 M HCl or 0.1 M NaOH. The final volume of the flasks was made up to 100 mL using autoclaved water. The flasks were then tightly sealed and placed in a constant temperature water bath at 45°C for 15 days with gentle shaking. Forty-five degree Celsius is an environmentally relevant temperature as it is common in tropical and subtropical areas, and has also been reported in temperate areas as the approximate temperature of the exposed soil surface on a day when the ambient air temperature is 25°C [25]. Therefore, the reaction products formed at 45°C were used for all of the detailed characterization using XRD, FTIR, total C, and C K-edge and Mn L-edge NEXAFS analyses in this study.

To investigate the effect of temperature on humification processes, selected systems (equimolar integrated pyrogallol/resorcinol-Maillard reaction systems with or without birnessite) were also incubated at 25°C for 15 days, and only the pH and pH + pE values of the systems and Mn concentration and visible absorbance of the supernatants were determined for comparison with the data obtained at 45°C (Table S1 in supplementary materials). The rest of the results presented in this study were obtained at 45°C.

The absence of microbial growth was verified by

culturing aliquots of selected samples at the end of the incubation period. Aerobic microbial growth was tested by culturing on Tryptocase Soy Agar (TSA) plates, while anaerobic microbial growth was tested on TSA plates in a BBL GasPak 150 Large Anaerobic System for a period of 5 and 9 days at 28°C [12]. All treatments were performed in triplicate.

2.2.2 Characterization of Reaction Systems at the End of the Incubation Period and Isolation of Humic Acids

At the end of the reaction period, the final pH and E_h of the solutions were measured. The samples were then centrifuged at 25,000 g for 40 min to separate the solid residue from the solution. The absorbance of the supernatant was measured between 400 and 600 nm on a UV-visible spectrophotometer (Beckman DU 650 spectrophotometer, Fullerton, CA, USA). The visible absorbance at 400 and 600 nm provides an indication of the extent of polymerization that has taken place in the reaction systems [26, 27]. The supernatant was diluted with water prior to absorbance determination and the values obtained were subsequently multiplied by the dilution factor.

The Mn content of the supernatant was determined by atomic absorption spectroscopy at 279.5 nm (Varian Spectra AA 220, Walnut Creek, CA, USA). The solid residue was repeatedly washed with water using centrifugation at 25,000 g for 40 min until the wash water was clear. These water extracts were collected and added to the supernatant. The washed residue was then freeze-dried. The combined washing and supernatant was then acidified to pH 1.0 using 6 M HCl and allowed to stand for 24 h to precipitate the humic acid (HA) fraction out of the solution [28]. The acidified suspensions were then centrifuged at 25000 g for 45 min to separate the HA fraction from the rest of the solution containing the fulvic acid (FA) fraction and non-humic substances fraction. The HA residue was then resuspended in a 0.1 M HCl and 0.3 M HF solution and shaken for 48 h. It was then centrifuged again as described above and dialyzed in 1000 molecular weight cut off dialysis tubing for 5 days in distilled deionized water until the water tested free of chloride ($AgNO_3$ test). The purified HA was then freeze-dried.

Selected HA samples which were used in the NEXAFS study were not purified using the HCl/HF treatment but were instead dialyzed immediately after being separated by acidification and centrifugation; it is not necessary to remove all the Mn, as its presence does not interfere with XAS studies. Furthermore, the HA samples without the HCl/HF treatment were used in the Mn L-edge NEXAFS studies to investigate the nature of Mn bonding in the samples.

2.3. Characterization of Reaction Products

2.3.1 Fourier Transform Infrared (FTIR) Spectroscopy

FTIR spectra of the washed and freeze-dried solid residues and purified HA fractions were obtained, by preparing KBr disks containing 1% w/w sample and running it on a Bruker Equinox 55 FTIR (Ettlingen, Germany) connected with a purge gas generator.

2.3.2 X-Ray Diffraction (XRD)

The solid residues, HA and unreacted biomolecules (pyrogallol, resorcinol, glucose and glycine) were examined by x-ray diffractometry on a Rigaku Rotaflex 200SU (Tokyo, Japan) with a rotating Fe anode and graphite monochromator. The samples were lightly ground and then mounted on glass slides by making a slurry of the ground sample with acetone and allowing it to dry. The scans were performed at 40 kV and 160 mA, from $2\theta = 4$ to 80°, at a step size of 0.02° at a scanning rate of 0.1° sec^{-1}.

2.3.3 Total Carbon Analysis

Total carbon analysis of the solid residues was performed by a dry combustion method on a Leco CR-12 Carbon Analyzer (Leco Corporation, St. Joseph, MI, U.S.A.) as described by Wang & Anderson [29].

2.3.4 Near Edge X-Ray Absorption Fine Structure (NEXAFS) Spectroscopy

The speciation of C and Mn was investigated in the solid residues and HA fractions from selected reaction systems using C K-edge and Mn L-edge NEXAFS at the Canadian Light Source (Saskatoon, SK, Canada) on the SGM (Spherical grating monochromator) beamline. A number of pure reference compounds (glucose, glycine, pyrogallol, $MnCO_3$, MnO, Mn_2O_3, MnO_2) and IHSS soil and peat HA standards were also examined. Samples investigated for Mn were lightly ground and mounted on carbon tape. Samples which were investigated for C were mounted on 99.99% indium (In) foil or gold (Au)-coated (~400 Å) silicon (Si) wafers. The solid residue samples were mounted on In by grinding the sample and then pressing the powder into the soft metal, scraping off the excess.

The relatively water-soluble samples, i.e., HAs and pure biomolecules, were mounted on the Au-coated Si wafers by making dilute solutions of the

samples in distilled deionized water and then placing a droplet on the wafer and allowing it to dry. An exit slit width of 20 μm and a dwell time of 0.1s were used to minimize damage due to exposure to radiation. These spectra were recorded by total electron yield (TEY) at an energy resolution of 0.1 eV. The Mn spectra were normalized to the TEY of I0 mesh gold, which is placed in front of the sample in the path of the beam. The C spectra were normalized to a clean Au-coated Si wafer so that the signals from C in the beamline and C contamination on the I0 mesh gold would not interfere with the signal from our samples [30]. Spectra obtained were analyzed using aXis2000 software [31]. The energy scale of the C and Mn spectra were internally calibrated using glycine and MnO, respectively based on calibrated values reported from previous studies [32, 33].

3. RESULTS

3.1. Characterization of Reaction Systems

3.1.1 Effect of Birnessite and Incubation Temperature

In all the reaction systems studied, no aerobic or anaerobic microbial growth was observed. Thus, all the processes studied were abiotic in nature.

The x-ray diffractogram of the synthesized birnessite showed the characteristic peaks at 7.21, 3.61 and 2.45 Å as reported by McKenzie [34]. The FTIR spectrum shows typical birnessite absorption bands at 3400, 1621, 509 and 466 cm^{-1}, as described by Potter & Rossman [35]. The Mn L-edge NEXAFS spectrum shows that the synthesized birnessite contains predominantly Mn(IV) with some Mn(III), which was also reported by Jokic et al. [8] using Mn K-edge X-ray absorption spectroscopy. The BET surface area was found to be 63 m^2g^{-1}, which is characteristic of synthetic birnessite [23].

The presence of birnessite significantly enhanced humification in the integrated polyphenol-Maillard reaction and polyphenol only systems, as the absorbances (degree of browning/polymerization) were much greater in the presence than in the absence of birnessite (Fig. 2). Enhancement of humification in the Maillard reaction system (glucose and glycine) by birnessite at 25°C and 45°C was reported by Jokic et al. [8]. Birnessite had the most dramatic enhancing effect on the degree of browning in the integrated polyphenol-Maillard systems (Fig. 2b and d) compared to the polyphenol only systems (Fig. 2a and c). The absorbance of the pyrogallol only system (Fig. 2a) showed the least response to the presence of birnessite. The pH of the reaction systems are controlled by two important processes, namely, oxidative polymerization, which results in the release of protons, and the reductive dissolution of birnessite, which consumes protons.

Temperature also has a substantial influence on browning reactions (Table S1). The visible absorbances of the pyrogallol- and resorcinol-Maillard reaction systems were much lower in the systems incubated at 25°C than at 45°C, both in the presence and absence of birnessite, indicating that increasing the temperature results in increased abiotic humification reactions. Similarly, Jokic et al. [12] studied the equimolar catechol-glucose-glycine system catalyzed by birnessite at 25°C and 45°C, and observed enhanced visible absorbance at the higher temperature.

3.1.2 Influence of the Molar Ratio of Polyphenol to Maillard Reagents on Reactions Systems Incubated at 45°C in the Presence of Birnessite

The pyrogallol-Maillard reaction systems had substantially lower final pH values than the resorcinol-Maillard systems (Fig. 3), which indicates a greater degree of net proton release as a result of oxidative polymerization and the reductive dissolution of birnessite in the pyrogallol systems than in the resorcinol systems. The first three increments of pyrogallol to Maillard reagents (1.25, 2.5 and 12.5 mmole of pyrogallol added) resulted in a net final pH that was higher than the starting pH of 7.00 (Fig. 3). When 2.5 mmole pyrogallol was added to Maillard reagents, there was a net decrease in the final pH of the reactions systems and this trend continued with increasing amounts of pyrogallol present. In contrast, increasing the amount of resorcinol added to Maillard reagents resulted in all the final pH values of the reactions systems being above the starting pH of 7.0 (Fig. 3), which were within a range of ± 0.5 pH units of Maillard reaction system's final of pH (8.08). The high final pH of the resorcinol-Maillard systems indicates that the reduction of birnessite, which consumes protons, was the dominant process affecting the pH of the reaction systems.

The concentration of Mn in the supernatants of the pyrogallol- and resorcinol-Maillard reaction systems showed significantly different trends (Fig. 4). Increasing the molar ratio of pyrogallol to Maillard reagents resulted in a dramatic decrease of detectable Mn up until a concentration of 2.5 mmole pyrogallol added, and then flattened off at the 50 and 100 mmole pyrogallol levels. The Mn concentration in the supernatant of the pyrogallol only system (1.6 mmole L^{-1}) was approximately 20 times lower than in the

equimolar pyrogallol-Maillard reaction system (31.8 mmole L^{-1}) and approximately 120 times lower than the Maillard reaction system (193 mmole L^{-1}).

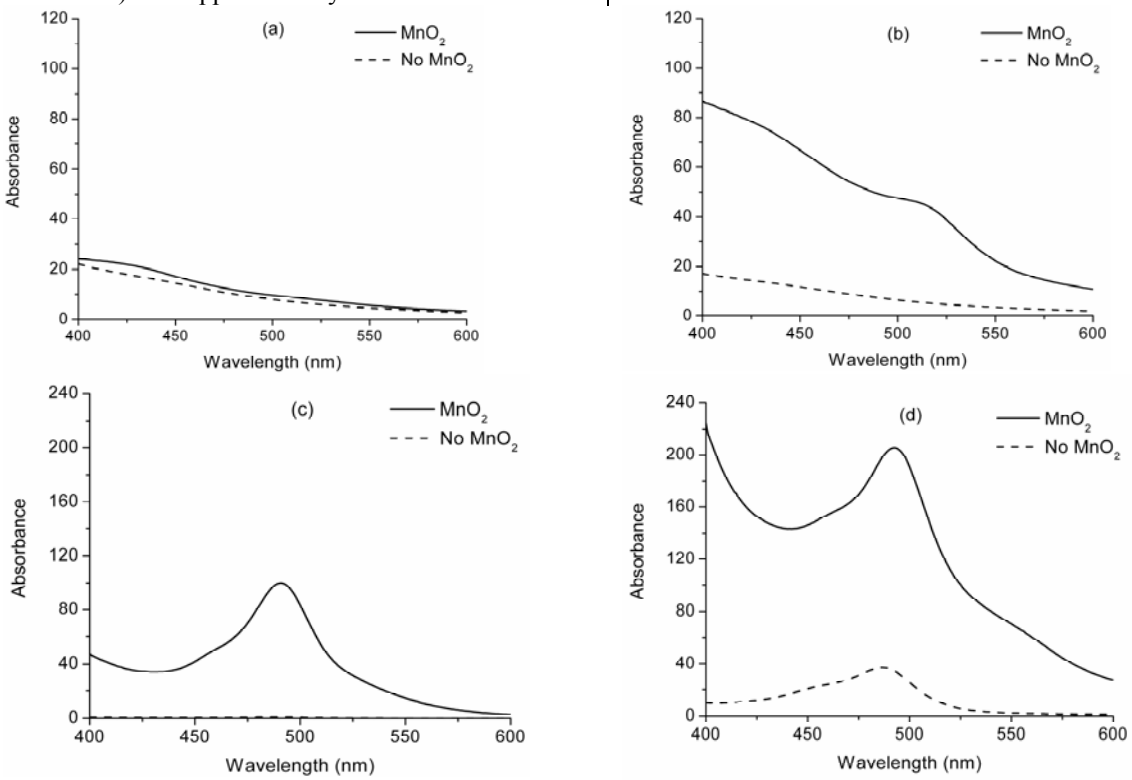

Figure 2 Comparison of the effect of birnessite on the absorbances of the supernatants of (a) the 50 mmole pyrogallol only system, (b) the integrated equimolar pyrogallol-Maillard system (50 mmole glucose + 50 mmole glycine + 50 mmole pyrogallol), (c) the 50 mmole resorcinol only system, (d) the integrated equimolar resorcinol-Maillard system (50 mmole glucose + 50 mmole glycine + 50 mmole resorcinol). The absorbances are scaled by the dilution factor.

Increasing the molar ratio of resorcinol to Maillard reagents initially resulted in a decrease in the concentration of Mn in the supernatant and then in a dramatic increase in the Mn concentration after the addition of 12.5 mmole or higher amounts of resorcinol. The Mn concentration in the supernatant of the resorcinol only system (32.7 mmole L^{-1}) was approximately 7 times lower than in the equimolar resorcinol-Maillard reaction system (216 mmole L^{-1}) and 6 times lower than the Maillard reaction system (193 mmole L^{-1}).

Both systems showed the trend of increased visible absorbance with increasing amount of polyphenol added (Fig. 5). The supernatant of the resorcinol-Maillard reaction systems had a greater overall visible absorbance than that of the pyrogallol-Maillard reactions systems. These results would appear contrasting to the pH data (Fig. 3), which indicated that compared with the resorcinol systems, the pyrogallol systems had a net greater degree of proton release as a result of oxidative polymerization of polyphenol and reduction of birnessite. However, as will be shown later, most of the polymers formed in the resorcinol systems remained suspended in the supernatants of these systems, whereas in the pyrogallol systems substantial amounts of the polymers precipitated and were found in the solid phase complexed with Mn(II).

3.2 Characterization of Reaction Products from Reaction Systems Incubated at 45°C in the Presence of Birnessite

3.2.1 The Solid Phase

X-ray diffraction. The solid residue from the Maillard reaction system (Fig. 6a) clearly shows the formation of crystalline $MnCO_3$ (rhodochrosite) with typical d-values of 3.67, 2.84, 2.18 and 1.76 Å [36]. There was a subsequent decrease in the amount and crystallinity

of the $MnCO_3$ formed with the introduction of pyrogallol (Fig. 6b) into the system. When the amount of pyrogallol in the pyrogallol-Maillard reaction system was increased to 25 mmole or higher, there was an abrupt disappearance of a crystalline reaction product (Fig. 6c-d). The diffractogram of the solid residue from the pyrogallol only reaction system (Fig. 6e) shows evidence of some poorly crystalline $MnCO_3$ (2.84 Å). The broad band at approximately 3.8 Å seen in the humic substances extracted from the supernatant of the 50 mmole pyrogallol integrated system (Fig. 6f), can clearly be seen in the 25 and 50 mmole pyrogallol integrated (Fig. 6c, d) and 50 pyrogallol only systems (Fig. 6e). This band was also observed by Wang and Huang [37] in the pyrogallol-derived humified solid residue as catalyzed by birnessite and other metal oxides, and is mainly attributed to the polyaromatic structure of humic substances [38].

The $MnCO_3$ formation trend in the integrated resorcinol-Maillard reaction systems (Fig. 7) is in contrast to that observed in the pyrogallol-Maillard reaction systems. In the resorcinol-Maillard reaction system, the addition of 2.5 mmole of resorcinol decreased the formation of $MnCO_3$; however, a further increase in the amount of resorcinol added promoted the formation of crystalline $MnCO_3$, as indicated by the intensity of the characteristic peaks of $MnCO_3$ (Fig. 7b-e).

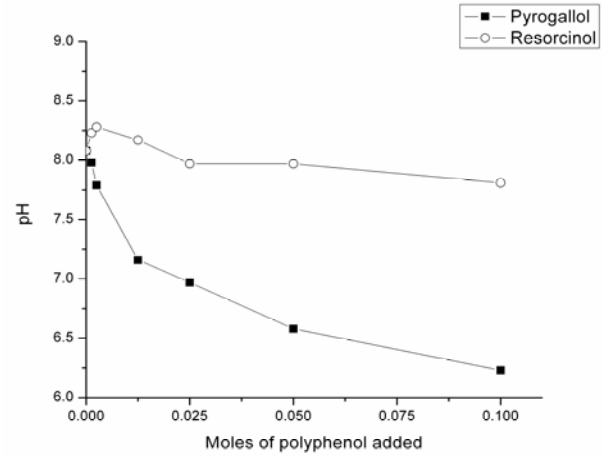

Figure 3 Comparison of the final pH of the integrated pyrogallol- and resorcinol-Maillard reaction systems, in the presence of birnessite, with increasing amount of polyphenol added. The pH value of the Maillard reaction system was the first point in the reaction system, i.e., 0 mole polyphenol added.

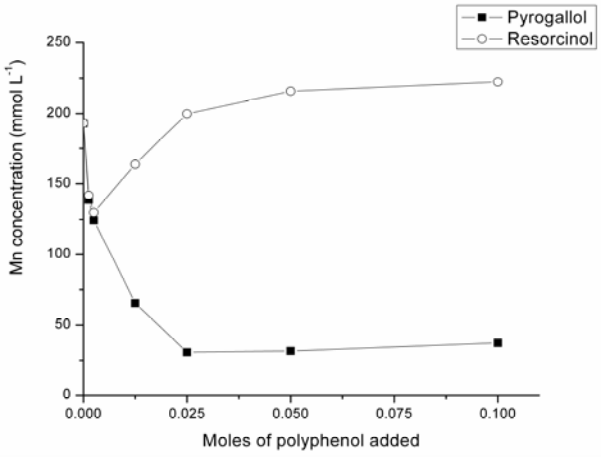

Figure 4 Comparison of Mn concentrations in the supernatants of the integrated pyrogallol- and resorcinol-Maillard reaction systems, in the presence of birnessite, with increasing amount of polyphenol added. The Mn concentration of the supernatant in the Maillard reaction system was the first point in the reaction system, i.e., 0 mole of polyphenol added.

The resorcinol only system (Fig. 7f) shows evidence of a number of relatively poorly crystalline Mn(II), Mn(III) and Mn(IV) mineral species: rhodochrosite ($MnCO_3$) at 3.67, 2.84 and 1.76 Å, hausmannite (Mn_3O_4, a mixed Mn(II)/Mn(III) oxide) at 2.77, 2.49 and 1.54 Å, manganite (γ-MnO(OH)) at 3.41, 2.64 and 2.28 Å, synthetic bixbyite (Mn_2O_3) at 4.94, 3.84, 2.72 and 1.66 Å, and birnessite (δ-MnO_2) at ~7.2, 3.61 and 2.41 Å [34]. The XRD results clearly show that resorcinol (Fig. 7f) is not able to reduce birnessite as easily as pyrogallol (Fig. 6e) or the Maillard reagents (Fig. 7a), and thus birnessite was not completely reduced to Mn(II) as in the pyrogallol and Maillard reaction systems.

The X-ray diffractograms of the unreacted biomolecules (pyrogallol, resorcinol, glycine and glucose) are shown in Fig. S1. The XRD spectra of the solid residues from the pyrogallol-Maillard and pyrogallol only systems (Fig. 6b-e) show that the resultant organic materials are heterogeneous and amorphous in nature, unlike the highly crystalline starting materials (Fig. S1).

Total carbon analysis. A comparison of the total C contents of the solid residues from the integrated pyrogallol- and resorcinol-Maillard reaction systems formed in the presence of birnessite is shown in Table 1. It is important to note that pure $MnCO_3$ has a lower total C content (10.4%) than humic substances, such as fulvic acid (FA) (45.7%) and humic acid (HA)

(56.2%) [39], or biomolecules such as glycine (31.9%), glucose (40.0%), pyrogallol (57.1%) or resorcinol (65.5%), which helps to explain the trends observed in the total C contents of the solid residues. The solid residues from the Maillard reaction had the lowest total C content (13.1%), which is close to that of pure $MnCO_3$, and this is strongly supported by the XRD data (Fig. 6a) indicating the presence of crystalline $MnCO_3$. Overall, the solid residues from the resorcinol-Maillard and resorcinol only systems had lower total C contents than the pyrogallol-Maillard and pyrogallol only systems, which again can be related to the extent of $MnCO_3$ formation in the systems as indicated by XRD (Fig. 6 and 7).

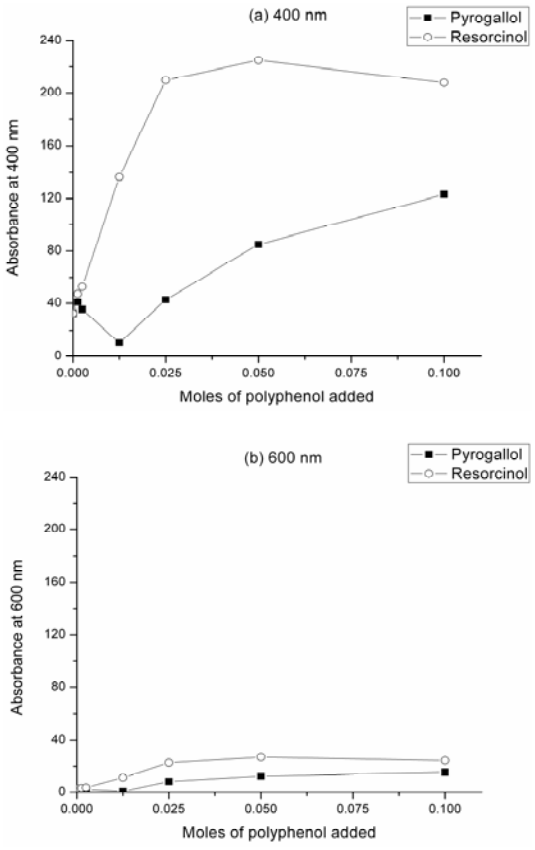

Figure 5 Comparison of the absorbances at 400 and 600 nm of the integrated pyrogallol- and resorcinol-Maillard reaction systems formed in the presence of birnessite with increasing amount of polyphenol added to the system. The absorbance of the supernatant in the Maillard reaction system was the first point in the reaction systems, i.e., 0 mole of polyphenol added. The absorbances are scaled by the dilution factor.

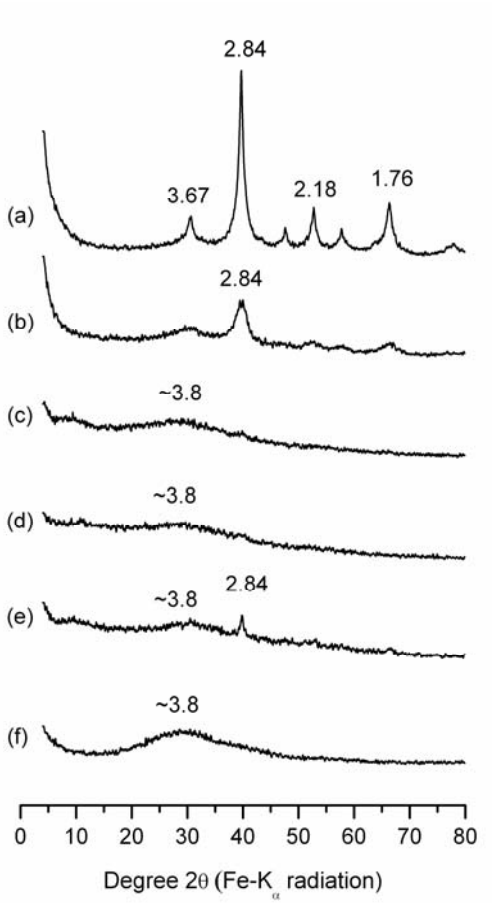

Figure 6 X-ray diffractograms of the solid residues formed in the presence of birnessite from the (a) Maillard reaction system; the integrated pyrogallol-Maillard reaction systems; with (b) 2.5 mmole pyrogallol, (c) 25 mmole pyrogallol, (d) 50 mmole pyrogallol; and (e) 50 mmole pyrogallol only; and (f) non-purified humic acid from the supernatant of the 50 mmole pyrogallol integrated system. D-spacings are indicated in Å.

The pyrogallol systems had an increasing percentage of C in the solid residues with increasing amount of pyrogallol added up to 25 mmole and thereafter the total C content remained virtually unchanged. This trend is in accord with the XRD data (Fig. 6a-d), which indicate an abrupt disappearance of $MnCO_3$ after 2.5 mmole of pyrogallol added in the integrated pyrogallol-Maillard systems and thus higher total C contents are expected from organic residues.

The resorcinol system shows an opposite trend after the 25 mmole resorcinol treatment, with the percentage of C decreasing in the solid residue. This is also in agreement with the XRD data (Fig. 7a-e) of the

resorcinol solid residues, which indicate increasing amounts of $MnCO_3$ formed with increasing amount of resorcinol in the system. The solid residue from the pyrogallol only system was shown to contain some $MnCO_3$ (Fig. 6e) and hence has a slightly lower total C content (Table 1) than the pyrogallol-Maillard systems, which contain trace amounts or no $MnCO_3$ (Fig. 6c-d). The resorcinol only system contained a lower total C content (15.3%) than the resorcinol-Maillard reaction systems (Table 1), which is probably a result of the significant amount of the Mn(II), Mn(III) and Mn(IV) oxides present (Fig. 7f).

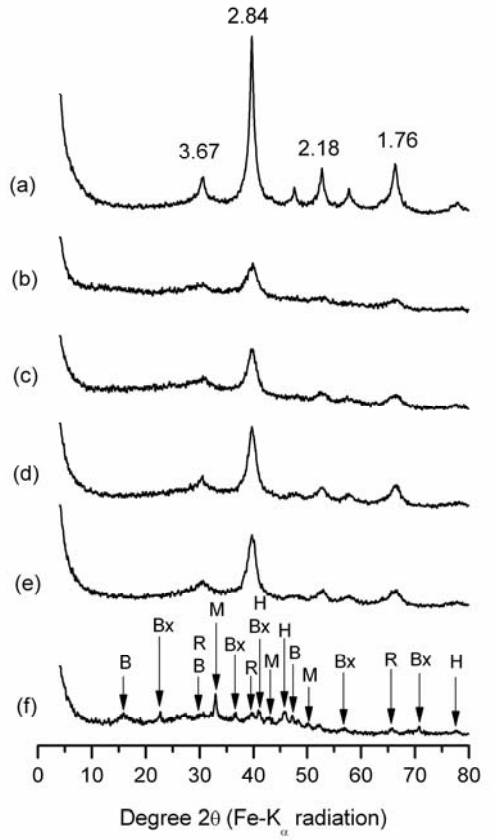

Figure 7 X-ray diffractograms of the solid residues formed in the presence of birnessite from (a) the Maillard reaction; the integrated resorcinol-Maillard reaction systems with: (b) 2.5 mmole resorcinol, (c) 25 mmole resorcinol, (d) 50 mmole resorcinol, (e) 100 mmole resorcinol; and (f) 50 mmole resorcinol only system. D-spacings are indicated in Å. B = birnessite (~7.2, 3.61, 2.41 Å), Bx = bixbyite (4.94, 3.84, 2.72, 1.66 Å), R = rhodochrosite (3.67, 2.84, 1.76 Å), M = manganite (3.41, 2.64, 2.28 Å), H = hausmannite (2.77, 2.49, 1.54 Å).

Table 1 Comparison of total carbon contents of solid residues from Maillard reaction, polyphenol-Maillard, and polyphenol only reaction systems formed in the presence of birnessite.

Treatment	Total C content (%)	
	Pyrogallol	Resorcinol
Maillard reaction (50 mmole glucose + 50 mmole glycine)	13.1	13.1
Polyphenol-Maillard reaction with 2.5 mmole polyphenol	19.8	22.0
Polyphenol-Maillard reaction with 25 mmole polyphenol	32.6	27.1
Polyphenol-Maillard reaction with 50 mmole polyphenol	32.1	20.9
Polyphenol-Maillard reaction with 100 mmole polyphenol	32.3	17.4
Polyphenol only (50 mmole polyphenol)	30.8	15.3

We could not differentiate between organic and inorganic C using the LECO analyzer as it is based on a dry combustion method and measures the CO_2 released at 841°C and 1100°C to distinguish between CO_2 released from organic C (841°C) and total C, i.e., inorganic C + organic C (1100°C). Manganese carbonate decomposes at temperatures above 200°C, which is substantially lower than the melting point of $CaCO_3$ (825°C) [40]. Calcium carbonate is considered the most common form of inorganic C in soils and sediments. Thus, the C from $MnCO_3$ would be included in the "organic C" fraction using the conventional dry combustion method.

Manganese L-edge NEXAFS. The Mn $L_{2,3}$-edges NEXAFS spectra of the solid residues from selected pyrogallol, resorcinol, and integrated pyrogallol- and resorcinol-Maillard systems, as well as, reference di-, tri- and tetra-valent Mn oxide and carbonate compounds are shown in Fig. 8. The Mn $L_{2,3}$-edges provide a sensitive fingerprint of the valence of Mn based on the absorption maxima (white lines) and shape of the spectra, and in some cases the site symmetry and ligands can also be identified [32, 41].

The maximum absorption peak of Mn(II) was observed at 640.3 eV, Mn(III) at 641.7 eV, and Mn(IV) at 644.0 eV, at the Mn L_3 edge. The shapes and photon energy values of the spectra of Mn species obtained in this study are in agreement with those of previous Mn $L_{2,3}$-edge NEXAFS studies [32, 41-43].

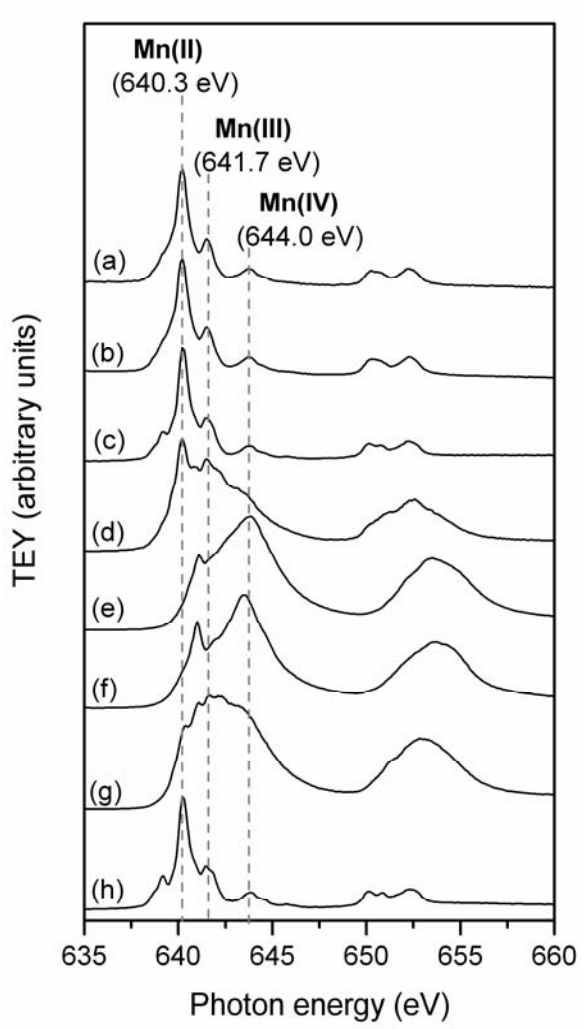

Figure 8 Mn $L_{2,3}$-edges NEXAFS spectra of solid residues formed in the presence of birnessite from selected integrated polyphenol-Maillard reaction and polyphenol only reaction systems, and pure Mn oxide and carbonate mineral standards: (a) equimolar pyrogallol-Maillard (b) pyrogallol only, (c) equimolar resorcinol-Maillard, and (d) resorcinol only reaction systems, and (e) MnO_2, (f) unreacted birnessite, (g) Mn_2O_3 and (h) $MnCO_3$. The dotted lines indicate the photon energy of the maximum absorption peak of Mn in divalent, trivalent or tetravalent states on the Mn L_3 edge.

The Mn $L_{2,3}$-edge spectra of the solid residues from the pyrogallol only, equimolar pyrogallol- and resorcinol-Maillard reaction systems show that Mn was principally in the divalent form in these systems (Fig. 8a-c). The spectra of the solid residues from the equimolar pyrogallol-Maillard reaction system (Fig. 8a) and pyrogallol only system (Fig. 8b) look similar to each other in that the minor absorption peak to the left of the maximum absorption peak is not resolved compared to pure $MnCO_3$ (Fig. 8h). This corresponds to Mn(II) that is covalently bonded to either O or N and in an octahedral environment [41], indicating that the Mn(II) in the solid residues from the pyrogallol systems (Fig. 8a, b) is covalently bonded to humic polymers. However, the spectrum of the solid residue of the equimolar resorcinol-Maillard system (Fig. 8c) looks more similar to that of pure $MnCO_3$ (Fig. 8h), which is in accord with the XRD (Fig. 7d) and FTIR (Fig. S3d) data, showing that the solid residue consisted predominantly of $MnCO_3$ and some humic substances. The resorcinol only system residue (Fig. 8d) appears to be a mixture of Mn(II) and Mn(III), with possibly a small amount of Mn(IV) present. This also is in agreement with the XRD data (Fig. 7f), which show the presence of a mixture of Mn(II), Mn(III) and Mn(IV) minerals.

Carbon K-edge NEXAFS. The C K-edge NEXAFS spectra of the solid residues from the Maillard reaction, pyrogallol only and pyrogallol-Maillard reaction systems are shown in Figure 9. Spectroscopic assignments are based on the absorption maxima of the reference compounds (glucose, glycine and pyrogallol) and on values reported by previous C NEXAFS studies [44-48]. The NEXAFS narrower and sharper core (C 1s) → π* transitions have been found to be the most useful for chemical analyses and identification of organic compounds due to their chemical sensitivity based on the chemical energy shifts [44].

The lowest absorption bands at around 284.0 eV usually correspond to molecules with low energy π* states, such as quinones [49]. Absorption bands near 285 eV are generally ascribed to C 1s (C-H) → $1\pi^*_{C=C}$ transitions [44, 46], which are characteristic of C=C unsaturation. The transitions of aromatic C bound to carbonyl (e.g. terephthalate species) tend to overlap with unsaturated aromatic C-H transitions due to the strong electronic interactions between the benzene π* density and carbonyl π* density, and are generally found in the 284.4-285.0 eV range [46]. The absorption bands near 286-288 eV are characteristic of functionalized aromatic groups C 1s (C-R) → $1\pi^*_{C=C}$ transitions (R = functional group), such as aromatic C bound to aldehyde (286.0 eV), ketone (286.4 eV), urea (286.4 eV), carbamate (286.6-286.8 eV), amine (286.8-286.9 eV), phenol (287.0-287.3 eV) and ester 287.1 (eV) groups [44-47]. Heterocyclic N compounds C 1s (C-N) → $1\pi^*_{C=C}$ transitions also occur in the ~286-287 eV range, e.g., pyridine (285.7 eV) and pyrrole (286.3 eV) [45, 47]. The C=N and

C≡N π* transitions usually occur around 286.3 eV [48]. Generally speaking, a stronger electron withdrawing substituent on the aromatic ring results in a higher energy shift of the C 1s (C-R) → $1\pi^*_{C=C}$ transition.

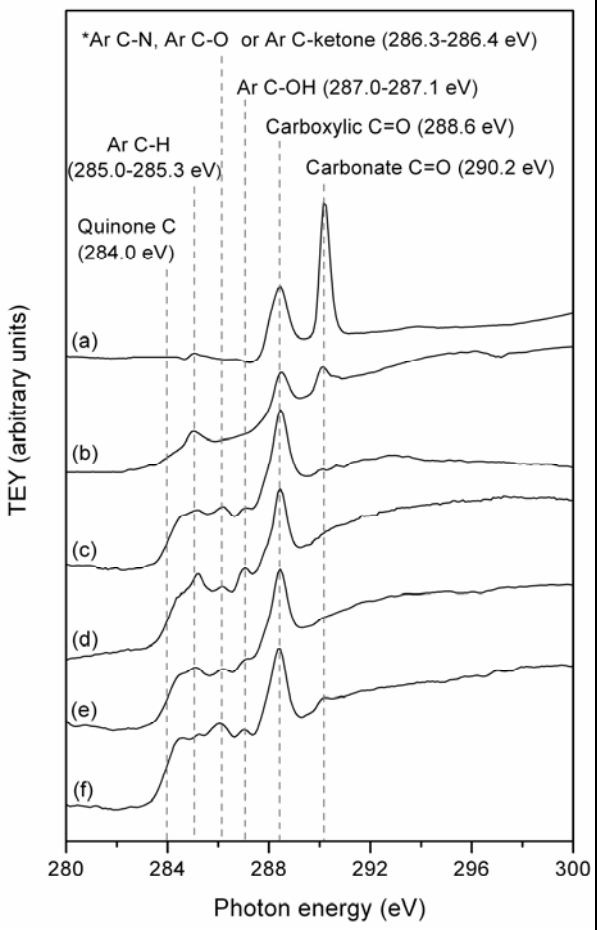

Figure 9 Carbon K-edge NEXAFS spectra of solid residues formed in the presence of birnessite in the Maillard reaction system (a); and selected pyrogallol-Maillard reaction systems with: (b) 2.5 mmole pyrogallol, (c) 25 mmole pyrogallol, (d) 50 mmole pyrogallol and (e) 100 mmole pyrogallol; and (f) 50 mmole pyrogallol only system. *Ar = aromatic.

The carbonyl C 1s (C-R) → $1\pi^*_{C=O}$ transitions usually occur between 286-291 eV, and can be used to distinguish between groups such as aldehydes (286.2-286.4 eV), ketones (286.6-286.8 eV), amide (287.8-288.2 eV), acetic/acetate (288.1-288.6 eV), urea (289.2-289.8 eV), carbamate (289.9.0-290.1 eV) and carbonate (290.2-290.6 eV) [44]. The main cause of the shifts observed in C 1s (C-R) → $1\pi^*_{C=O}$ transitions is the inductive effect of the neighboring atoms on the carbonyl C 1s binding energy [44].

Low-lying σ* orbitals also provide valuable information in identifying aliphatic functionalities. Saturated aliphatic C exhibits C 1s (C-H) → σ^*_{C-H} transitions in the 287.1-287.9 eV range, while aliphatic alcohol C 1s (C-H) → σ^*_{C-O} transitions are found shifted to a higher energy in the 289.2-289.5 eV range [45].

The C K-edge NEXAFS spectrum of the solid residue from the Maillard reaction system (Fig. 9a) clearly shows that carbonate C=O (290.2 eV) and carboxylic C=O (acetic/acetate, i.e, aliphatic) (288.6 eV) are the dominant functionalities present, which is in agreement with the FTIR data (Fig. S3a). As shown by the XRD data (Fig. 6b-d), increasing the molar ratio of pyrogallol to Maillard reagents resulted in a decrease of $MnCO_3$ in the integrated pyrogallol-Maillard reaction system (Fig. 9b-e). Furthermore, it clearly can be seen that the organic substances in the solid residues of the pyrogallol-Maillard and pyrogallol only systems (Fig. 9c-f) are dominated by aliphatic carboxylic C=O functionalities (288.6 eV). They also contain some aromatic functionalities, including quinone (284.0 eV), aromatic C-H (285.0-285.3 eV), possibly aromatic C bound to ketone, O or N (including heterocyclic N) (286.4 eV), and phenolic groups (287.0-287.1 eV). It is also interesting to note that the dominant functional group of glucose, which is aliphatic alcohol groups (289.4 eV), is not evident in any of the spectra from the solid residues.

FTIR Spectroscopy. The FTIR spectra of the solid residues from the Maillard reaction, polyphenol only and selected polyphenol-Maillard reaction systems are shown in Fig. S2 and S3. Comprehensive assignments of the absorption peaks are provided in Table S2. The FTIR spectra of the solid residues from these systems are in agreement with XRD and NEXAFS data of these systems (Fig. 6, 8 & 9). The FTIR spectra also show that organic substances in solid residues of the resorcinol-Maillard reaction systems (Fig. S3b-e), appear very similar to those found in the solid residue of Maillard reaction system (Fig. S3a). The organic substances found in these systems appear to be dominated by carboxylic functional groups, predominantly in the deprotonated state, as indicated by symmetric (1594 cm^{-1}) and antisymmetric (1408 cm^{-1}) COO^- stretch absorption bands. In contrast to the resorcinol-Maillard reaction systems (Fig. S3b-e), the resorcinol only system contained humic substances with significant aromatic character, as indicated by the strong absorption band at 1613 cm^{-1} (Fig. S3f).

3.2.2 Humic Acid Fraction Isolated From Supernatant

Carbon K-edge NEXAFS. The C K-edge NEXAFS spectra of the peat and soil HA standard materials of the International Humic Substance Society (IHSS) and the HA isolated from the supernatant of selected reaction systems (Maillard reaction, pyrogallol- and resorcinol-Maillard, pyrogallol and resorcinol only) are shown in Fig. 10.

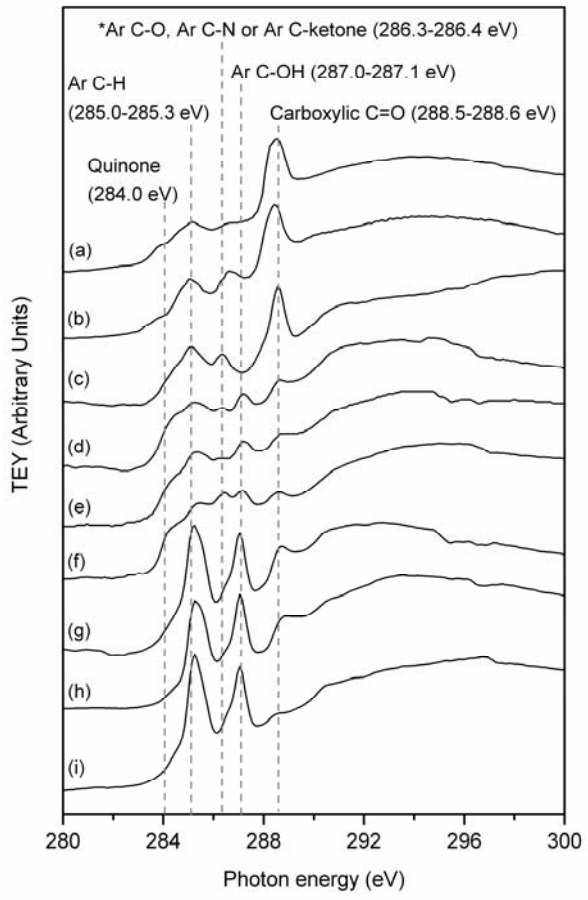

Figure 10 Carbon K-edge NEXAFS spectra of the IHSS (a) soil and (b) peat humic acids, and the humic acids extracted from the supernatants of reaction systems catalyzed by birnessite: (c) Maillard reaction; pyrogallol-Maillard reaction with: (d) 50 mmole pyrogallol and (e) 100 mmole pyrogallol; (f) 50 mmole pyrogallol only; resorcinol-Maillard reaction with: (g) 50 mmole resorcinol and (h) 100 mmole resorcinol; and (i) 50 mmole resorcinol only system. *Ar = aromatic.

The HA isolated from the supernatant of the Maillard reaction system were dominated by carboxylic type C (288.5-288.6 eV), and also contained aromatic C-H functionalities (285.0-285.3 eV) and possibly either aromatic ketone, aromatic C bound to N (including heterocyclic N) or other aromatic C bound to O functional groups (286.3-286.4 eV) (Fig. 10c). The spectra of the pyrogallol-Maillard and pyrogallol only systems (Fig. 10d-f) show more broad and less defined peaks than the Maillard (Fig. 10c) and resorcinol systems (10g-i), indicating that the HA formed in the pyrogallol systems is more heterogeneous in nature than the Maillard reaction and resorcinol systems.

The pyrogallol systems were dominated by aromatic C-H, phenolic and carboxylic C (Fig. 10d-f). The peaks of the quinone (284.0 eV) and aromatic C bound to ketone, N or O (286.3-286.4 eV) are more prominent in the HAs from pyrogallol systems (Fig. 10d-f) than resorcinol systems (Fig. 10g-i). Increasing the amount of the pyrogallol in the pyrogallol-Maillard reaction system from 50 to 100 mmole did not result in a significant change in the nature of the humic acid (Fig 10d and e).

The HAs from the pyrogallol only system HA (Fig. 10f) appears to have a stronger presence of aromatic C bound to ketone or O than the HAs from the pyrogallol-Maillard reaction systems (Fig 10d and e). The resorcinol system HA spectra (Fig.10g-i) show sharper peaks, indicative of more homogeneous reaction products that are dominated by aromatic C-H and phenolic and aliphatic carboxylic C=O functional groups. Increasing the amount of resorcinol in the resorcinol-Maillard system from 50 to 100 mmole resulted in a decrease in the intensity of the aliphatic carboxylic C peak at 288.5-288.6 eV (Fig. 10g and h). The resorcinol only system was also dominanted by aromatic C-H and phenolic peaks and contained very little carboxylic C (Fig. 10i). The pyrogallol only system (Fig. 10f) contained more carboxylic C than the resorcinol only system (Fig. 10i).

The C K-edge NEXAFS spectra of the IHSS soil and peat HAs (Fig. 10a and b) look basically similar to the HAs isolated from the Maillard reaction and pyrogallol-Maillard reaction systems in that they contain quinone, aromatic C, functionalized aromatic C and carboxylic C. Similar to the spectra of the natural HAs (Fig. 10a and b), the spectrum of the HA from the Maillard reaction system (Fig. 10c) is also dominated by carboxylic C (288.5-228.6 eV). The soil HA (Fig. 10a) appears to have lower intensity of the peak between aromatic C-OH and aromatic ketone, aromatic C-N or C-O compared to the peat HA (Fig. 10b).

FTIR Spectroscopy. The FTIR spectra of the HA isolated from the supernatants of the Maillard reaction, selected polyphenol-Maillard reaction, and polyphenol only reaction systems are shown in Figures S4 and S5. Comprehensive assignments of the absorption bands are provided in Table S3. The FTIR results of the HAs from these systems support the findings of C NEXAFS analyses of these systems (Fig. 10c-i).

4. DISCUSSION

4.1. Characterization of the Reaction Systems at the End of the Reaction Period

Effect of Birnessite and Temperature. It is well-established that birnessite significantly accelerates the polymerization of polyphenols [26] as well as the polycondensation of polyphenols and amino acids [27]. The surfaces of redox active metal oxides such as birnessite are very reactive in promoting the polymerization of phenolic compounds. They can act as Lewis acids by accepting electrons from hydroxyphenolics, leading to the formation of highly reactive semiquinone radicals that readily undergo coupling reactions with other semiquinones, phenolics, amino acids or existing humus [11, 50].

Electron transfer between polyphenolics and Mn oxides is facilitated by direct surface complexation of the phenolic OH-group or carboxylic group of the aromatic compound to the surface of the metal oxide. Subsequently, the reduced metal is released into solution, uncovering more metal oxide sites for reaction [18, 51]. Matocha et al. [52] studied the kinetics of reduction of birnessite by catechol (*o*-dihydroxy-benzene) and confirmed that the reaction occurs and is controlled by precursor surface complex formation, as the electron transfer itself is very rapid. They also confirmed that release of Mn(II) into solution was directly related to o-quinone production.

Jokic et al. [7] reported that the reaction between D-glucose and glycine is very slow at room temperature due to the high activation energy barrier. Jokic et al., [8] showed that birnessite can significantly accelerate the Maillard reaction between glucose and glycine. Furthermore, Jokic et al., [12] demonstrated that birnessite significantly enhances humification in the integrated catechol-glucose-glycine system. Our results show that birnessite is able to significantly enhance the degree of browning in the pyrogallol- and resorcinol-glucose-glycine reaction systems (Fig. 2b, d), as well as moderately enhancing the degree of browning in the resorcinol only system (Fig. 2c).

The pyrogallol only system appeared to show the least response to the presence of birnessite (Fig. 2a). This could be, in part, due to the highly reactive nature of pyrogallol, which enables it to polymerize itself quite readily without the presence of a catalyst such as birnessite. More important is the fact that a substantial amount of humified organic material is found in the solid phase of the birnessite-catalyzed pyrogallol system, based on evidence from the Mn $L_{2,3}$-edge (Fig. 8b) and C K-edge NEXAFS (Fig. 9f) and FTIR (Fig. S2f) data of the solid residues.

Thus, the humic substances in the solid phase are not taken into account by visible absorbance readings of the supernatant. The reaction systems in the presence of birnessite had lower final pH + pE (indication of dissolved oxygen in the system) values at the end of the reaction period than the controls (Table S1). This is attributed to increased oxidative polymerization of polyphenols which consumes oxygen, as indicated by the visible absorbance values.

The systems in the presence of birnessite had higher final pH values (Table S1) due to the reductive dissolution of birnessite by the biomolecules glucose, glycine and or pyrogallol/resorcinol, which resulted in the consumption of protons (Eq. 1).

$$MnO_2 + 4H^+ + 2e^- \rightarrow Mn^{2+} + 2H_2O \qquad (1)$$

Temperature was shown to significantly affect the humification processes, as indicated by the visible absorbance, pH and pH + pE values of the integrated pyrogallol- and resorcinol-Maillard reactions both in the presence and absence of birnessite (Table S1). Jokic et al. [12] also showed that increasing temperature enhanced the extent of humification in the catechol-glucose-glycine reaction. They found that the E_4/E_6 ratio of humic acid isolated from the supernatant of the system incubated at 25°C was lower (4.46) than that of humic acid produced at 45°C (7.43), indicating that the humic substances produced at 45°C are more aliphatic in nature and less condensed due to enhanced cleavage at a higher temperature.

Effect of the Molar Ratio of Polyphenol to Maillard Reagents in Reactions Systems Incubated at 45°C in the Presence of Birnessite. Stone and Morgan [18] found that polyhydroxyphenolics with OH groups in the *ortho* or *para* positions can form direct surface complexes with Mn (III, IV) oxides much more readily than polyphenols with OH groups in the *meta* position. They determined the relative second-order rate constants for the dissolution of Mn (III, IV) oxide at pH 7.2 by various polyhydroxyphenolics, including catechol (*o*-OH group)–2 x 10^1 M^{-1} s^{-1}, hydroquinone (*p*-OH group)–2.33 x 10^0 M^{-1} s^{-1} and resorcinol (*m*-OH

group)–4.9 x 10^{-3} M^{-1} s^{-1}. Direct surface complexation significantly enhances electron transfer reactions, and subsequently the dissolution of Mn oxide and the formation of free radicals (semi-quinones), which readily participate in polymerization reactions. Thus, pyrogallol with three hydroxyl groups all in the *ortho* position to one another is able to react with birnessite far more readily than resorcinol which has two OH groups in the *meta* position. Shindo [20] clearly showed that pyrogallol reaction with birnessite yields more humic polymers than resorcinol reaction with birnessite.

This is indicated in our data by the steady decrease of pH with increasing moles of pyrogallol added in the reactions systems (Fig. 3). Pyrogallol, which is able to participate in direct electron transfer reactions more readily, has a greater polymerization reactivity and thus more protons are generated in pyrogallol-containing systems. Resorcinol, with an OH group in the *meta* position, is not able to participate in direct electron transfer reactions as readily, which means a lower oxidative polymerization reactivity and fewer protons generated. However, in the resorcinol-Maillard reaction system, glucose (a reducing sugar) and glycine are able to carry out the reductive dissolution of birnessite [8], which consumes protons and ultimately controls the final pH of the systems. This explains why the final pH values of the resorcinol-Maillard reaction systems were very close to that of the Maillard reaction (Fig. 3). Furthermore, it is clear that in the resorcinol only system (Fig. 8d), the extent of reduction of Mn in birnessite to Mn(II) is substantially less than the pyrogallol only, pyrogallol- and the resorcinol-Maillard reactions systems (Fig. 8a-c), as shown by the presence of a mixture of Mn(II), Mn(III) and Mn(IV) oxides in the solid phase of the resorcinol only system (Fig. 7f and 8d).

The pyrogallol-Maillard reaction systems with the lowest amounts of pyrogallol (1.25 and 2.5 mmole) to Maillard reagents (50 mmole glucose + 50 mmole glycine) showed a net increase from the starting pH of 7.00 to the pH values of 7.8 to 8.0 which were close to that of the Maillard reactions system (Fig. 3). This indicates that the reductive dissolution of birnessite predominantly driven by the Maillard reaction is the dominant process controlling the final pH. Further increase of the amount of pyrogallol added resulted in a net drastic decrease in the pH of the systems, indicating the oxidative polymerization of biomolecules as the dominant process. This is also confirmed by the visible absorbance of the supernatants of pyrogallol-Maillard reaction systems (Fig. 5), where initially there was a decrease in the visible absorbance, but above the 1.25 mmole pyrogallol treatment the increasing pyrogallol added resulted in a significant and steady increase in absorbance. This indicates that the addition of a sufficient amount of pyrogallol to Maillard reagents results in a large increase in the degree of humification. This trend of increase of the absorbance with increasing molar ratios of resorcinol to Maillard reagents was also observed (Fig. 5).

Trends in the Mn concentration (Fig 4) and visible absorbance (Fig. 5) of the supernatants from the pyrogallol- and resorcinol-Maillard reaction systems cannot be properly explained without first discussing the nature of the humic substances formed in these systems, which follows below.

4.2. Characterization of Reaction Products from Reaction Systems Incubated at 45°C in the Presence of Birnessite

Humic Substances. Another important impact of the relative ability of pyrogallol and resorcinol to form direct surface complexes with birnessite is aromatic ring cleavage. Wang and Huang [19] clearly showed that pyrogallol is far more easily cleaved by nontronite (Fe-bearing smectite) than the diphenols catechol (*o*-dihydroxybenzene) or hydroquinone (*p*-dihydroxy-benzene). This is related to their relative ability to form direct surface complexes with the mineral surface. Wang and Huang [19] also concluded that the greater the ease of ring cleavage of a polyphenol, the more CO_2 is released and the more aliphatic fragments were incorporated into the resultant humic substances.

Furthermore, Wang and Huang [22] demonstrated substantial ring cleavage of pyrogallol by birnessite. Increased ring cleavage and the resultant increase in aliphatic fragment incorporation lead to humic substances with more aliphatic nature and more COOH functional groups [37]. These groups have a much higher affinity for binding divalent cations, such as dissolved Mn(II), than phenolic OH groups, and it is well known that COOH functionalities give humic substances most of their cation complexing capacity [1]. The logarithm of the stability constant (K) (ionic strength = 0.1 μ, 25°C) of the complex of glycine and Mn(II) is +2.80, whereas for catechol and Mn(II) log K is -14.70 [53].

This indicates that the humic substances produced in the pyrogallol containing systems, which possess more carboxylic functionalities, are able to sorb Mn(II) to a much greater extent than polymers with more aromatic or phenolic character. Increased metal complexation would eventually result in the coprecipitation of humic substances out of solution due to decreased solubility as a result of increase in molecular size and charge neutrality [54].

Direct evidence for this is provided by the FTIR and the C and Mn NEXAFS spectra of the solid residues and the HAs isolated from the supernatant of the pyrogallol-Maillard reaction and pyrogallol only systems in the present study. It is clear that the humified organic substances found in the solid residues are dominated by carboxylic functional groups (Fig. S2 and 9), compared to the HAs from the supernatant (Fig. S4 and 10), which possess a significant aromatic and phenolic character.

The Mn L-edge NEXAFS spectra of the equimolar pyrogallol-Maillard reaction and pyrogallol only systems provide further evidence that Mn(II) in the solid residue is covalently bonded to either O or N (Fig. 8a and b). It appears that the solid residues of the pyrogallol-Maillard reactions system containing 25 mmole pyrogallol or above (Fig. S2c-e) consisted completely of humified organic materials complexed with Mn, as there is no evidence of $MnCO_3$ or any other Mn mineral. This is also indicated by the Mn L-edge NEXAFS spectra (Fig. 8a). The chemical fractionation of HA from a humic gleysol by divalent and trivalent metal cations was demonstrated by Christl and Kretzschmar [55] using C 1s NEXAFS spectroscopy. They concluded that the cation-induced coagulation of humic acid resulted in the preferential removal of humic acid with functional groups involved in metal-cation binding, in particular, aliphatic carboxylic groups. The conclusions from this afore-mentioned study [55] using natural humic acid agree with our findings.

Recently, it has been proposed that humic substances are collections of diverse, relatively low molar mass components that are associated by hydrophobic interactions and hydrogen bonds [56]. This view has questioned the formation of humic substances by polymerization of phenolic compounds. Our study of the polyphenol-Maillard reaction clearly shows that a significant amount of aliphatic material is formed due to ring cleavage of phenols as well as the incorporation of Maillard reagents into the humic acid fraction through condensation reactions. Furthermore, the NEXAFS spectra show that the humification products of biomolecules and IHSS standard humic substances also contain substantial aromatic character (Fig. 9 and 10). Therefore, the data indicate that polycondensation reactions and the formation of aliphatic fragments through aromatic ring cleavage proceed concomitantly. The present findings would partially account for the aliphaticity of humic substances in soils [1, 57] and the variation of their characteristics, including carboxylic group contents, with soils in different climatic zones [57].

Resorcinol is not able to readily form a direct surface complex with birnessite due to an OH group in the *meta* position [18]. Therefore it is unable to readily participate in electron transfer reactions like pyrogallol and thus does not undergo substantial ring cleavage or polymerization through direct electron transfer. It is possible that electron transfer might occur through outer-sphere reactions [18] or due to reaction with Maillard reagents, particularly glycine, or Maillard reaction products, which include a range of aromatic compounds including various polyphenols [13], heterocyclic N [9], and highly reactive furfural compounds [5].

It is evident from the C K-edge NEXAFS spectra of the HAs from the supernatant of the resorcinol-Maillard reaction (Fig 10g and h) that these HAs contained more carboxylic functionalities than the HAs from the resorcinol only system (Fig. 10i), which would be due to the influence of Maillard reagents in the system. Decreased ring cleavage in the resorcinol system would mean that the resultant humic substances would have less aliphatic fragment incorporation compared to pyrogallol. This is very evident from the C NEXAFS spectra of the HAs from the pyrogallol and resorcinol systems, where the pyrogallol systems' HAs (Fig. 10d-f) are far more heterogeneous and poorly defined compared to resorcinol systems' HAs, which are dominated by aromatic C-H and phenolic C-OH functionalities (Fig. 10g-i).

In sharp contrast to the pyrogallol-Maillard systems in which $MnCO_3$ was absent when the amount of pyrogallol added was 25 mmole or higher (Fig 6c and d), the solid residues of the resorcinol-Maillard systems consisted predominantly of $MnCO_3$ (Fig. 7 b-e) and some Maillard reaction-type humic substances (Fig. S3). This indicates that the bulk of the humic polymers produced in the resorcinol-Maillard reaction system remain in the supernatant and are not precipitated in the solid residue complexed with Mn(II) as in the pyrogallol containing systems. This reasoning is in accord with the Mn L-edge NEXAFS spectra of the solid residues of the integrated resorcinol- and pyrogallol-Maillard reaction systems; the data show that Mn(II) was bound to carbonate in the former system and covalently bound to organics in the latter system (Fig. 8a and c). This further substantiates the view that the strongly aromatic/phenolic polymers formed in a resorcinol-Maillard reaction system have a lower affinity for Mn(II) and hence remain in the supernatant. These findings also provide an explanation for the contrasting trends observed in the Mn concentration (Fig. 4) of the supernatant of the resorcinol- and pyrogallol-Maillard reaction systems, and the substantially higher dissolved Mn concentration and visible absorbance values in the former than the latter

(Fig. 5).

The results indicate less Mn(II) sorption and more humic polymers in the supernatant in the resorcinol-Maillard reaction systems compared with the pyrogallol-Maillard system. Therefore, the ability of the polyphenols to form direct surface complexes with birnessite not only affects the extent of their oxidative polymerization reactions, but also the nature of the humic substances formed and ultimately their partition in the solution and solid phases in the system, whether remaining in solution or coprecipitating with metals out of solution.

Manganese carbonate. The formation of $MnCO_3$ in the polyphenol-Maillard reaction system as influenced by the structure and functionality of polyphenols and their molar ratio to Maillard reagents is clearly shown by the XRD, Mn L-edge NEXAFS and FTIR data (Fig. 6, 7, 8, and S2, S3). It has been shown previously that CO_2 is produced during the oxidation of glycine [21, 58], catechol [59], pyrogallol [22] and glucose [12] by birnessite. Carbon dioxide released from these biomolecules dissolves in solution to form carbonic acid (Eq. 2):

$$CO_2 + H_2O \leftrightarrow H_2CO_3 \quad (\text{Log } K = -1.46)\ [60] \qquad (2)$$

Carbonic acid dissociates to form bicarbonate and eventually carbonate depending on the pH of the solution (Eq. 3 and 4):

$$H_2CO_3 \leftrightarrow H^+ + HCO_3^- \quad (\text{Log } K = -6.36)\ [60] \qquad (3)$$

$$HCO_3^- \leftrightarrow H^+ + CO_3^{2-} \quad (\text{Log } K = -10.33)\ [60] \qquad (4)$$

The partial pressure of CO_2 in the atmosphere is usually 0.0003 atm. However, in a water-logged system the partial pressure can be as high as 0.3 atm, thus resulting in much higher CO_3^{2-} concentrations [60]. The CO_2 released from the oxidation of biomolecules (glucose, glycine, pyrogallol and resorcinol) would enhance the partial pressure of CO_2 and dissolution of CO_2 in water to form H_2CO_3. Reduction of birnessite by the biomolecules resulted in substantial release of Mn (Fig. 4) as Mn(II) in solution as shown in previous studies using EPR spectrometry [8, 22, 52]. Thus, $MnCO_3$ (rhodochrosite) can form in the system when the activity product of Mn^{2+} and CO_3^{2-} (Eq. 5) exceeds the K_{sp} of $MnCO_3$ (1.8×10^{-18}) [60]:

$$Mn^{2+}\,(aq) + CO_3^{2-}\,(aq) \leftrightarrow MnCO_3\,(s) \qquad (5)$$

Therefore, the biomolecule-induced formation of $MnCO_3$ is considered as a mechanism of the formation of rhodochrosite, as the CO_2 is derived from oxidation of biomolecules. The XRD (Fig. 6a, b and e, and 7b-e), Mn L-edge NEXAFS (Fig. 8c) and FTIR (Fig. S2 a and b, and S3 a-e) data show the formation of $MnCO_3$ in the reaction systems. Okita et al.[61] hypothesized that the $MnCO_3$ deposit at Molango, Mexico formed due to the reduction of manganese oxides by organic materials and that the organic-derived CO_2 resulted in negative $\delta^{13}C$ values and manganese carbonate formation. Furthermore, rhodochrosite-like $MnCO_3$ has been identified as one of the dominant Mn-bearing minerals in a naturally occurring palustrine emergent wetland [62]. The present findings provide experimental evidence substantiating the hypothesis of the biogenic formation of $MnCO_3$ deposits and for interpreting the presence of rhodochrosite-like $MnCO_3$ in wetlands.

Increasing the pyrogallol concentration in the pyrogallol-Maillard reaction systems resulted in less $MnCO_3$ formation (Fig. 6a-d). This is, in part, attributed to the lower solution pH values (Fig. 3), due to increased oxidative polymerization reactions, which decrease the CO_3^{2-} concentration in solution. In addition, the larger amounts of humic polymers apparently had an inhibitory effect on $MnCO_3$ formation due to perturbation of the crystallization of pure $MnCO_3$ (Fig. 6a-d) and also the competing effect of humic polymers for Mn^{2+} through complexation as indicated in the drastic decrease in the solution Mn concentration with increase of the amount of pyrogallol present in the systems (Fig. 4). The high solution pH (Fig. 3) and Mn concentration (Fig. 4) of the resorcinol-Maillard reaction systems favor the formation of $MnCO_3$ in the solid residues.

The XRD data (Fig. 7b-e) indicate that increasing the resorcinol concentration in the resorcinol-Maillard reaction system promotes the formation of crystalline $MnCO_3$. The FTIR spectra of the solid residues (Fig. S3b-e) also clearly show that the formation of Maillard-reaction organic products in solid residues of the resorcinol-Maillard reaction systems decreased with increasing amounts of resorcinol added to the system. This could be due to the formation of more aromatic/phenolic polymers in the resorcinol-Maillard reaction system (Fig. 10g-i) with increasing amounts of resorcinol added to the system, which has a lower affinity for Mn(II) and thus increased the concentration of Mn(II) in solution (Fig. 4) and the amount of polymers in the supernatant (Fig 5). At the same time, increasing the resorcinol concentration in the resorcinol-Maillard reaction system would result in increased competition for glycine by resorcinol versus the Maillard reaction. This would, in turn, result in less Maillard reaction products, which are rich in carboxylic functional groups and thus have a

high affinity for Mn(II).

Therefore, the reaction conditions in the resorcinol system are more favorable for the formation of $MnCO_3$. In the resorcinol only system, the birnessite was only partially reduced to both Mn(III) and Mn(II) (Fig. 8d); the formation of $MnCO_3$ is hindered due to the partial dissolution of birnessite and competitive formation of a number of relatively poorly crystalline Mn(II) and Mn(III) mineral species (Fig. 7f).

CONCLUSIONS

The significance of linking the polyphenol and Maillard reactions as promoted by birnessite (δ-MnO_2) into an integrated humification pathway has been demonstrated by Jokic et al. [12] using a system containing catechol, glucose and glycine. However, the role of structure and functionality of polyphenols in influencing the integrated polyphenol-Maillard reaction humification pathway remained to be uncovered.

The results obtained in the present study demonstrate that there is a significant difference in the reactivity of pyrogallol and resorcinol in the integrated polyphenol-Maillard reaction humification pathway. Pyrogallol (1,2,3-trihydroxybenzene), with three OH groups in the *ortho* position, is able to form direct surface complexes with birnessite far more readily than resorcinol (1,3-dihydroxybenzene), with two OH groups in the *meta* position. This significantly affects the extent of direct electron transfer reactions, such as reductive dissolution of birnessite, and oxidative polymerization and cleavage of biomolecules, which, in turn, affects the nature of the humic substances formed. The humic acids formed in the pyrogallol-Maillard reaction (glucose-glycine) systems are more heterogeneous in nature and contain more aliphatic and carboxylic fragments than those from the resorcinol-Maillard reaction systems, which contain more aromatic polymers. Partitioning of organic material in the solution and solid phases occurs, whereby the more aliphatic/carboxylic polymers are found precipitated in the solid phase due to stronger complexing with Mn(II), whereas more aromatic polymers are present in the supernatant due to their lower affinity for Mn(II). Increasing the molar ratio of pyrogallol or resorcinol to Maillard reagents enhances humification and results in the formation of humic substances with more aromatic character.

The structure and functionality of pyrogallol and resorcinol and their molar ratio to Maillard reagents also affect inorganic C formation. The biomolecule-induced formation of rhodochrosite ($MnCO_3$) was observed in the polyphenol-Maillard reaction humification pathway as a result of the oxidation of the biomolecules glucose, glycine, pyrogallol and resorcinol by birnessite. The integrated pyrogallol-Maillard reaction systems contain the least $MnCO_3$ and are more enriched in humic substances in the solid phase than the integrated resorcinol-Maillard reaction systems. There is an increase in the amount of crystalline $MnCO_3$ with increasing amount of resorcinol present in the reaction system. The opposite trend is observed in the integrated pyrogallol-Maillard reaction humification pathway.

Our data show that the position and/or number of -OH groups on the benzene ring of polyphenols and the molar ratio of polyphenol to Maillard reagents substantially affect not only the degree of humification and nature of humic polymers formed but also the extent of $MnCO_3$ formation, which is a competing reaction to the genesis of humic substances. The findings obtained in this study are of fundamental significance in understanding the importance of the nature and abundance of biomolecules in influencing abiotic humification and carbonate formation in natural environments. The results of this study also have relevance to treating phenolic wastes using Mn oxides or soils, as the chemical structures of phenolic compounds significantly affect their ability to be polymerized or cleaved (detoxified), or their reaction products to be complexed with metals.

ACKNOWLEDGEMENTS

This study was supported by a Discovery Grant (GP 2383-Huang) from the Natural Sciences and Engineering Research Council of Canada. The Tuition Scholarship awarded to A.G. Hardie from the University of Saskatchewan is much appreciated. We would like to thank Edwige Ottero from the Department of Chemistry, University of Saskatchewan, for her assistance in preparing Au-coated Si wafers used as sample mounts for the C K-edge NEXAFS study. The NEXAFS research described in this work was performed at the Canadian Light Source (CLS), which is supported by NSERC, NRC, CIHR, and the University of Saskatchewan. We thank the SGM beamline scientists at the CLS, Robert Blyth and Tom Regier, for their assistance.

REFERENCES

[1] Stevenson FJ. *Humus chemistry: Genesis, composition, reactions*. 2nd ed. New York: Wiley, 1994.

[2] Huang PM. Soil mineral-organic matter-microorganism interactions: Fundamentals and impacts. *Adv. Agron.,* 2004, 82: 391-472.
[3] Schaumann GE. Review articles. Soil organic matter beyond molecular structure Part I: Macromolecular and supramolecular characteristics. *J. Plant Nutr.,* 2006, 169: 145-156.
[4] Maillard LC. Formation de matières humiques par action de polypeptides sur sucres. *C.R. Acad. Sci*., 1913, 156: 148-149.
[5] Ikan R, Rubinsztain Y, Nissenbaum A, Kaplan IR. Geochemical aspects of the Maillard reaction. In: Ikan R ed. *The Maillard Reaction: Consequences for the Chemical and Life Sciences.* Chichester: Wiley, 1996.
[6] Anderson HA, Bick W, Hepburn A, Stewart M. Nitrogen in humic substances. In: Hayes MHB, MacCarthy P, Malcolm RL, Swift RS eds. *Humic Substances II. In Search of Structure.* Chichester: Wiley-Interscience, 1989, 223-253.
[7] Jokic A, Zimpel Z, Huang PM, Mezey PG. Molecular shape analysis of a Maillard reaction intermediate. *SAR and QSAR Environ. Res*., 2001, 12: 297-307.
[8] Jokic A, Frenkel AI, Vairavamurthy MA, Huang PM. Birnessite catalysis of the Maillard reaction: Its significance in natural humification. *Geophys. Res. Lett.,* 2001, 28: 3899-3902.
[9] Jokic A, Schulten H-R, Cutler JN, Schnitzer M, Huang PM. A significant abiotic pathway for the formation of unknown nitrogen in nature. *Geophys. Res. Lett*., 2004, 31: L05502.
[10] Bollag J-M, Dec J, Huang PM. Formation mechanisms of complex organic structures in soil habitats. *Adv. Agron.,* 1998, 63: 237-266.
[11] Huang PM. Abiotic catalysis. In: Sumner ME ed. *Handbook of Soil Science*. Boca Raton: CRC Press, 2000, B302-B332.
[12] Jokic A, Wang MC, Liu C, Frenkel AI, Huang PM. Integration of the polyphenol and Maillard reactions into a unified abiotic pathway for humification in nature: The role of δ-MnO_2. *Org. Geochem.,* 2004, 35: 747-762.
[13] Haffenden LJW, Yaylayan VA. Mechanism of formation of redox-reactive hydroxylated benzenes and pyrazine in ^{13}C-labled glycine/D-glucose model systems. *J. Agric. Food Chem*., 2005, 53: 9742-9746.
[14] Kögel-Knabner I. The macromolecular organic composition of plant and microbial residues as inputs to soil organic matter. *Soil Biol. Biochem.*, 2002, 34: 139-162.
[15] Filley TR, Cody GD, Goodell B, Jellison J, Noser C, Ostrofsky A. Lignin demethylation and polysaccharide decomposition in spruce sapwood degraded by brown rot fungi. *Org. Geochem.*, 2002, 33: 11-124.
[16] Martin JP, Haider K. Microbial activity in relation to soil humus formation. *Soil Sci*., 1971, 111: 54-63.
[17] McBride MB. Oxidation of 1,2- and 1,4-dihydroxybenzenes in aerated aqueous suspensions of birnessite. *Clays Clay Miner.,* 1989, 37: 470-486.
[18] Stone AT, Morgan JJ. Reduction and dissolution of manganese(III) and manganese(IV) oxides by organics. 2. Survey of the reactivity of organics. *Environ. Sci. Technol.*, 1984, 18: 617-624.
[19] Wang MC, Huang PM. Structural role of polyphenols in influencing the ring cleavage and related chemical reactions as catalyzed by nontronite. In: Senesi N, Miano TM eds. *Humic Substances in the Global Environment and Implications on Human Health.* Amsterdam: Elsevier, 1994, 173-180.
[20] Shindo H. Relative effectiveness of short-range ordered Mn(IV), Fe(III), Al and Si oxides in the synthesis of humic acids from phenolic compounds. *Soil Sci. Plant Nutr.,* 1992, 38: 459-465.
[21] Wang MC, Huang PM. Cleavage of ^{14}C-labled glycine and its polycondensation with pyrogallol as catalyzed by birnessite. *Geoderma,* 2005, 124: 415-426.
[22] Wang MC, Huang PM. Ring cleavage and oxidative transformation of pyrogallol catalyzed by Mn, Fe, Al and Si oxides. *Soil Sci.,* 2000, 165: 934-942.
[23] McKenzie RM. The synthesis of birnessite, cryptomelane, and some other oxides and hydroxides of manganese. *Mineral Magazine*, 1971, 38: 493-502.
[24] Wang TSC, Wang MC, Feng YL, Huang PM. Catalytic synthesis of humic substances by natural clays, silts and soils. *Soil Sci.,* 1983, 135: 350-360.
[25] Jury WA, Gardener WR, Gardener WH. *Soil physics*. 5th Ed. New York: Wiley, 1991.
[26] Shindo H, Huang PM. Role of Mn(IV) oxide in abiotic formation of humic substances in the environment. *Nature,* 1982, 298: 363-365.
[27] Shindo H, Huang PM. Significance of Mn(IV) oxide in abiotic formation of organic nitrogen complexes in natural environments. *Nature*, 1984, 308: 57-58.
[28] Swift RS. Organic matter characterization. In: Sparks DL ed. *Methods of Soil Analysis. Part 3.*

Chemical Methods. Madison: Soil Science Society of America, 1996, 1018-1020.

[29] Wang D, Anderson DW. Direct measurement of organic carbon content in soils by the Leco CR-12 carbon analyzer. *Comm. Soil Sci. Plant Anal.*, 1998, 29: 15-21.

[30] Watts B, Thomsen L, Dastoor PC. Methods in carbon K-edge NEXAFS: Experiment and analysis. *J. Electron Spectrosc.*, 2006, 151: 105-201.

[31] Hitchcock AP, Morin C, Zhang X, Araki T, Dynes JJ, Stover H, Brash JL, Lawrence JR, Leppard GG. Soft X-ray spectromicroscopy of biological and synthetic polymer systems. *J. Electron Spectrosc.*, 2005, 144-147: 259-269.

[32] Garvie LAJ, Craven AJ. High-resolution parallel electron energy-loss spectroscopy of Mn $L_{2,3}$-edges in inorganic manganese compounds. *Phys. Chem. Minerals*, 1994, 21: 191-206.

[33] Boese J, Osanna A, Jacobsen C, Kirz J. Carbon edge XANES of amino acids and peptides. *J. Electron Spectrosc.*, 1997, 85: 9-15.

[34] McKenzie RM. Manganese oxides and hydroxides. In: Dixon JB, Weed SB eds. *Minerals in Soil Environments*. Madison: Soil Science Society of America, 1989, 439-465.

[35] Potter RM, Rossman GR. The tetravalent manganese oxides: Identification, hydration, and structural relationships by infrared spectroscopy. *Am. Mineral.*, 1979, 64: 1199-1218.

[36] International Centre for Diffraction Data. *Powder diffraction file: Minerals search manual for experimental patterns*. Newton Square: JCPDS - International Centre for Diffraction Data, 1971.

[37] Wang MC, Huang PM. Characteristics of pyrogallol-derived polymers formed by catalysis of oxides. *Soil Sci.*, 2000, 165: 737-747.

[38] Pollack SS, Lentz H, Ziechmann W. X-ray diffraction study of humic acids. *Soil Sci.*, 1971, 112: 318-324.

[39] Schnitzer M. Humic substances: chemistry and reactions. In: Schnitzer M, Khan SU eds. *Soil Organic Matter*. Amsterdam: Elsevier, 1978, 1-64.

[40] Perry DL, Phillips SL. *Handbook of inorganic compounds.* Boca Raton: CRC Press, 1995.

[41] Grush MM, Chen J, Stemmler TL, George SJ, Ralston CY, Stibrany RT, Gelasco A, Christou G, Gorun SM, Penner-Hahn JE, Cramer SP. Manganese L-edge X-ray absorption spectroscopy of manganese catalase from *Lactobacillus plantarum* and mixed valence manganese complexes. *J. Am. Chem. Soc.*, 1996, 118: 65-69.

[42] Cramer SP, de Groot FMF, Ma Y, Chen CT, Sette F, Kipke CA, Eichhorn DM, Chen MK, Armstrong WH, Libby F, Christou G, Brooker S, McKee V, Mullins OC, Fuggle JC. Ligand field strengths and oxidation states from manganese L-edge spectroscopy. *J. Am. Chem.* Soc., 1991, 113: 7937-7940.

[43] Gilbert B, Frazer BH, Belz A, Conrad PG, Nealson KH, Haskel D, Lang JC, Srajer G, Stasio GD. Multiple scattering calculations of bonding and X-ray absorption spectroscopy of manganese oxides. *J. Phys. Chem.* A., 2003, 107: 2839-2847.

[44] Urquhart SG, Ade H. Trends in the carbonyl core (C 1s, O 1s) → p*C=O transition in the near-edge X-ray absorption fine structure spectra of organic molecules. *J. Phys. Chem. B*, 2002, 106: 8531-8538.

[45] Dhez O, Ade H, Urquhart SG. Calibrated NEXAFS spectra of some common polymers. *J. Electron Spectrosc.*, 2003, 128: 85-96.

[46] Cooney RR, Urquhart SG. Chemical trends in the near-edge X-ray absorption fine structure of monosubstituted and *para*-bisubstituted benzenes. *J. Phys. Chem. B.*, 2004, 108: 18185-18191.

[47] Hitchcock AP, Mancini DC. Gas-phase core excitation database (online). *http://unicorn.mcmaster.ca/corex/cedb-title.html.*

[48] Myneni SCB. Soft X-ray electron spectroscopy and spectromicroscopy studies of organic molecules in the environment. In: Fenter PA, Rivers ML, Sturchio NC, Sutton SR eds. *Applications of Synchrotron Radiation in Low-Temperature Geochemistry and Environmental Sciences.* Washington: Mineralogical Society of America, 2002: Vol. 49, 485-558.

[49] Francis JT, Hitchcock AP. Inner-shell spectroscopy of *para*-benzoquinone, hydroquinone, and phenol - distinguishing quinoid and benzoid structures. *J. Phys. Chem.*, 1992, 96: 6598-6610.

[50] Dec J, Bollag J-M. Phenoloxidase-mediated interactions of phenols and anilines with humic materials. *J. Environ. Qual.*, 2000, 29: 655-676.

[51] Stone AT, Morgan JJ. Reduction and dissolution of manganese(III) and manganese(IV) oxides by organics. 1. Reaction with hydroquinone. *Environ. Sci. Technol.*, 1984, 18: 450-456.

[52] Matocha CJ, Sparks DL, Amonette JE, Kukkadapu RK. Kinetics and mechanisms of

birnessite reduction by catechol. *Soil Sci. Soc. Am. J.*, 2001, 65: 58-66.
[53] Martell AE, Smith RM. *NIST standard reference database 46. NIST critically selected stability constants of metal complexes.* Gaithersburg: NIST Standard Reference Data, 2004.
[54] McBride MB. *Environmental chemistry of soils*. London: Oxford University Press, 1994.
[55] Christl I, Kretzschmar R. C-1s NEXAFS spectroscopy reveals chemical fractionation of humic acid by cation-induced coagulation. *Environ. Sci. Technol.,* 2007, 41: 1915-1920.
[56] Sutton R, Sposito G. Molecular structure in soil humic substances: the new view. *Environ. Sci. Technol.*, 2005, 39: 9009-9014.
[57] Schnitzer M. Recent findings on the characterization of humic substances extracted from soils from widely differing climatic zones. *Soil Organic Matter Studies II*. Vienna: IAEA Bulletin, 1977, 77-101.
[58] Wang MC, Huang PM. Polycondensation of pyrogallol and glycine and the associated reactions as catalyzed by birnessite. *Sci. Total Environ.,* 1987, 62: 435-442.
[59] Majecher EM, Chorover J, Bollag J-M, Huang PM. Evolution of CO_2 during birnessite-induced oxidation of ^{14}C-labeled catechol. Soil *Sci. Soc. Am. J*., 2000, 64: 157-163.
[60] Lindsay WL. *Chemical equilibria in soils*. New York: Wiley, 1979.
[61] Okita PM, Maynard JB, Spiker EC, Force ER. Isotopic evidence for organic matter oxidation by manganese reduction in the formation of stratiform manganese carbonate ore. *Geochim. Cosmochim. Acta,* 1988, 52: 2679-2685.
[62] La Force MJ, Hansel CM, Fendorf S. Seasonal transformations of manganese in a palustrine emergent wetland. *Soil Sci. Soc. Am. J.,* 2002, 66: 1377-1389.

AES7529b

© Northeastern University, 2007